Inorg. Chem. **2005**, *44*, 896–903

Structure, Electrochemistry, and Magnetism of the Iron(III)-Substituted Keggin Dimer, $[Fe_6(OH)_3(A\text{-}\alpha\text{-}GeW_9O_{34}(OH)_3)_2]^{11-}$

Li-Hua Bi,[†] Ulrich Kortz,*[,†] Saritha Nellutla,[‡] Ashley C. Stowe,[‡] Johan van Tol,[‡] Naresh S. Dalal,*[,‡] Bineta Keita,[§] and Louis Nadjo*[,§]

School of Engineering and Science, International University Bremen, P. O. Box 750 561, 28725 Bremen, Germany, Department of Chemistry and Biochemistry, Florida State University and National High Magnetic Field Laboratory and Center for Interdisciplinary Magnetic Resonance, Tallahassee, Florida 32306-4390, and Laboratoire de Chimie Physique, UMR 8000, CNRS, Equipe d'Electrochimie et Photoélectrochimie, Université Paris-Sud, Bâtiment 350, 91405 Orsay Cedex, France

Received September 14, 2004

The iron(III)-substituted tungstogermanate $[Fe_6(OH)_3(A\text{-}\alpha\text{-}GeW_9O_{34}(OH)_3)_2]^{11-}$ (**1**) has been synthesized and characterized by IR, elemental analysis, SQUID magnetometry, electron paramagnetic resonance (EPR), and electrochemistry. Single-crystal X-ray analysis was carried out on $Cs_4Na_7[Fe_6(OH)_3(A\text{-}\alpha\text{-}GeW_9O_{34}(OH)_3)_2]\cdot 30H_2O$, which crystallizes in the monoclinic system, space group $C_{2/m}$, with $a = 36.981(4)$ Å, $b = 16.5759(15)$ Å, $c = 16.0678(15)$ Å, $\beta = 95.311(3)°$, and $Z = 4$. Polyanion **1** consists of two (A-α-GeW_9O_{34}) Keggin moieties linked via six Fe^{3+} ions, leading to a double-sandwich structure. The equivalent iron centers represent a trigonal prismatic Fe_6 fragment, resulting in virtual D_{3h} symmetry for **1**. Electrochemistry studies revealed that **1** is stable in solution from pH 3 to at least pH 7. In pH = 3 media the reduction of the six Fe^{3+} centers was featured by a single voltammetric wave for most supporting electrolytes used. In that case, whatever the scan rate from 1000 mV·s^{-1} down to 2 mV·s^{-1}, no splitting of the single Fe-wave of **1** was observed. The acetate medium induced a partial splitting of the wave, and this separation is enhanced with increasing pH. Remarkable efficiency of **1** in the electrocatalytic reduction of nitrite, nitric oxide, and nitrate is demonstrated. Magnetic susceptibility (χ) measurements indicate a diamagnetic ($S_T = 0$) ground state, with an average $J = -12$ cm^{-1} and $g = 2.00$. EPR studies confirm that the ground state is indeed diamagnetic, since the EPR signal intensity steadily decreases without any line broadening as the temperature is lowered and becomes unobservable below about 50 K. The signal is a single broad peak at all frequencies (90–370 GHz), ascribed to the thermally accessible excited states. Its g_{iso} is 1.992 51, as expected for a high-spin Fe^{3+}-containing species, and supports the χ data analysis.

Introduction

Polyoxometalates (POMs) have attracted increasing attention in recent years because of their exciting structural variety combined with a multitude of properties.[1a−d] The possibility of tuning POM size, shape, charge density, acidity, redox potential, stability, and solubility characteristics leads to potential applications of these compounds in analytical sciences, materials science, catalysis, and medicine and in the emerging areas of bio- and nanotechnology.[1e−j] Although POMs have been known for about 200 years, a large number of novel polyoxoanions with unexpected shapes and sizes

* To whom correspondence should be addressed. Fax: +49-421-200 3229. E-mail: u.kortz@iu-bremen.de.
[†] International University Bremen.
[‡] Florida State University.
[§] Université Paris-Sud.

(1) (a) Pope, M. T. *Heteropoly and Isopoly Oxometalates*; Springer-Verlag: Berlin, 1983. (b) Pope, M. T.; Müller, A. *Angew. Chem., Int. Ed. Engl.* **1991**, *30*, 34. (c) *Polyoxometalates: From Platonic Solids to Anti-Retroviral Activity*; Pope, M. T., Müller, A., Eds.; Kluwer: Dordrecht, The Netherlands, 1994. (d) *Chemical Reviews*; Hill, C. L., Ed.; American Chemical Society: Washington, DC, 1998; Vol. 98, Issue 1 (Thematic Issue on Polyoxometalates). (e) *Polyoxometalate Chemistry: From Topology via Self-Assembly to Applications*; Pope, M. T., Müller, A., Eds.; Kluwer: Dordrecht, The Netherlands, 2001. (f) *Polyoxometalate Chemistry for Nano-Composite Design*; Yamase, T., Pope, M. T., Eds.; Kluwer: Dordrecht, The Netherlands, 2002. (g) Pope, M. T. *Compr. Coord. Chem. II* **2003**, *4*, 635. (h) Hill, C. L. *Compr. Coord. Chem. II* **2003**, *4*, 679. (i) *Polyoxometalate Molecular Science*; Borrás-Almenar, J. J., Coronado, E., Müller, A., Pope, M. T., Eds.; Kluwer: Dordrecht, The Netherlands, 2004. (j) Casan-Pastor, N.; Gomez-Romero, P. *Front. Biosci.* **2004**, *9*, 1759.

10.1021/ic048713w CCC: $30.25
Published on Web 01/25/2005

are still being discovered. Over the past decade or so a number of very large POMs have attracted considerable attention. Müller *et al*. have reported on several mixed-valence polyoxomolybdates with amazing sizes (up to 368 Mo atoms) and a variety of shapes (sphere, basket, ring, lemon, and hedgehog).[2] A lanthanide-containing heteropolytungstate with 148 tungsten atoms has been prepared by Pope *et al*.,[3] and the largest self-condensed heteropolytungstate known to date (containing 65 W atoms) was reported by Kortz *et al*.[4]

Transition metal-substituted POMs constitute the largest subclass of polyanions, and such species are of particular interest in catalysis and magnetism. Formation of multi-transition metal-substituted POMs can lead to molecules with high-spin ground states.[5c,d,6] On the other hand, activation of dioxygen or hydrogen peroxide by transition metal-substituted POMs for the efficient and selective oxidation of small organic molecules is already well-established.[7] Within the class of transition metal-substituted POMs, the sandwich-type compounds represent the largest subclass.[5] To date the Weakley-, Hervé-, Krebs-, and Knoth-type sandwich structures can be distinguished. Synthesis of such compounds is usually accomplished by reaction of a transition metal ion (e.g. Cu^{2+}, Mn^{2+}) with the appropriate lacunary POM precursor (e.g. $[AsW_9O_{33}]^{9-}$, $[GeW_9O_{34}]^{10-}$, and $[P_2W_{15}O_{56}]^{12-}$). Incorporation of up to four paramagnetic transition metal ions has been accomplished routinely,[5c,d] but examples of sandwich-type polyanions with greater than four paramagnetic metal centers are still rare.[5a]

This applies also to the class of iron-substituted POMs, which is of particular interest (a) for catalytic applications due to the easily accessible $Fe^{2+/3+}$ redox couple and (b) for magnetic applications due to the large number of unpaired electrons in high-spin $Fe^{2+/3+}$ combined with the possibility of forming spin-crossover magnetic molecular materials.[8] Some structures of Fe^{3+}-containing POMs have been reported predominantly by Hill *et al*., and interestingly most of them are of the Weakley sandwich type including mixed-metal derivatives (e.g. $[Fe_4(H_2O)_2(B\text{-}\alpha\text{-}PW_9O_{34})_2]^{6-}$, $[Mn_2(H_2O)_2\text{-}Fe_2(B\text{-}\alpha\text{-}P_2W_{15}O_{56})_2]^{14-}$).[9] Kortz *et al*. reported on the Krebs-type derivatives $[Fe_4(H_2O)_{10}(\beta\text{-}XW_9O_{33})_2]^{n-}$ ($n = 6$, X = As^{III}, Sb^{III}; $n = 4$, X = Se^{IV}, Te^{IV}).[10] Tézé *et al*. isolated the dimeric polyanion $[\{\alpha\text{-}SiW_{10}O_{37}Fe_2(OH)_2\}_2]^{12-}$ with an unprecedented structure.[11] Mizuno *et al*. reported on the monomeric, Keggin-type species $[\gamma(1,2)\text{-}SiW_{10}\{Fe(OH_2)\}_2\text{-}O_{38}]^{6-}$.[12] Finally, Jin *et al*. reported on the structure of the dimeric tungstophosphate $[Fe_4(OH)_4(PW_{10}O_{37})_2]^{10-}$.[13] Many of the above iron-containing POMs and some others have been investigated for their magnetic,[14] catalytic,[15] and electrocatalytic[9a,16] properties.

Interestingly, all of the above structurally characterized POMs are based on tungstophosphate, -silicate, and -arsenate fragments. To date, no iron-substituted tungstogermanate has been reported. Very recently, Kortz *et al*. described the synthesis, characterization, and magnetic properties of the Weakley-type sandwich polyanions $[M_4(H_2O)_2(B\text{-}\alpha\text{-}GeW_9O_{34})_2]^{12-}$ (M = Mn^{2+}, Cu^{2+}, Zn^{2+}, Cd^{2+}).[5c]

Following our core synthetic interests to synthesize POMs with catalytic, electrocatalytic, and magnetic properties, we decided to study in detail interaction of Fe^{3+} ions with the trilacunary $[A\text{-}\alpha\text{-}GeW_9O_{34}]^{10-}$ precursor.[17]

(2) Müller, A.; Roy, S. *Coord. Chem. Rev.* **2003**, *245*, 153, and references therein.

(3) Wassermann, K.; Dickman, M. H.; Pope, M. T. *Angew. Chem., Int. Ed. Engl.* **1997**, *36*, 1445.

(4) Kortz, U.; Savelieff, M. G.; Bassil, B. S.; Dickman, M. H. *Angew. Chem., Int. Ed.* **2001**, *40*, 3384.

(5) Representative examples include the following and references therein: (a) Bi, L.-H.; Kortz, U. *Inorg. Chem.* **2004**, *43*, 7961. (b) Bi, L.-H.; Reicke, M.; Kortz, U.; Keita, B.; Nadjo, L.; Clark, R. J. *Inorg. Chem.* **2004**, *43*, 3915. (c) Kortz, U.; Nellutla, S.; Stowe, A. C.; Dalal, N. S.; Rauwald, U.; Danquah, W.; Ravot, D. *Inorg. Chem.* **2004**, *43*, 2308. (d) Kortz, U.; Nellutla, S.; Stowe, A. C.; Dalal, N. S.; van Tol, J.; Bassil, B. S. *Inorg. Chem.* **2004**, *43*, 144. (e) Keita, B.; Mbomekalle, I. M.; Nadjo, L.; Anderson, T. M.; Hill, C. L. *Inorg. Chem.* **2004**, *43*, 3257. (f) Ritorto, M. D.; Anderson, T. M.; Neiwert, W. A.; Hill, C. L. *Inorg. Chem.* **2004**, *43*, 44. (g) Limanski, E. M.; Drewes, D.; Krebs, B. *Z. Anorg. Allg. Chem.* **2004**, *630*, 523. (h) Laronze, N.; Marrot, J.; Hervé, G. *Inorg. Chem.* **2003**, *42*, 5857.

(6) Representative examples include the following and references therein: (a) Stowe, A. C.; Nellutla, S.; Dalal, N. S.; Kortz, U. *Eur. J. Inorg. Chem.* **2004**, 3792. (b) Tasiopoulos, A. J.; Vinslava, A.; Wernsdorfer, W.; Abboud, K. A.; Christou, G. *Angew. Chem., Int. Ed.* **2004**, *43*, 2117.

(7) Hill, C. L. *Angew. Chem., Int. Ed.* **2004**, *43*, 402, and references therein.

(8) Representative examples include the following and references therein: (a) Sato, O. *Acc. Chem. Res.* **2003**, *36*, 692. (b) Ouahab, L. *Coord. Chem. Rev.* **1998**, *178*, 1501. (c) Ksenofontov, V.; Gaspar, A. B.; Niel, V.; Reiman, S.; Real, J. A.; Gütlich, P. *Chem. Eur. J.* **2004**, *10*, 1291.

(9) (a) Mbomekalle, I. M.; Keita, B.; Nadjo, L.; Neiwert, W. A.; Zhang, L.; Hardcastle, K. I.; Hill, C. L.; Anderson, T. M. *Eur. J. Inorg. Chem.* **2003**, 3924. (b) Anderson, T. M.; Zhang, X.; Hardcastle, K. I.; Hill, C. L. *Inorg. Chem.* **2002**, *41*, 2477. (c) Zhang, X.; Duncan, D. C.; Chen, Q.; Hill, C. L. *Inorg. Synth.* **2002**, *33*, 52. (d) Limanski, E. M.; Piepenbrink, M.; Droste, E.; Burgemeister, K.; Krebs, B. *J. Cluster Sci.* **2002**, *13*, 369. (e) Anderson, T. M.; Hardcastle, K. I.; Okun, N.; Hill, C. L. *Inorg. Chem.* **2001**, *40*, 6418. (f) Zhang, X.; Chen, Q.; Duncan, D. C.; Lachicotte, R. J.; Hill, C. L. *Inorg. Chem.* **1997**, *36*, 4381. (g) Zhang, X.; Chen, Q.; Duncan, D. C.; Campana, C. F.; Hill, C. L. *Inorg. Chem.* **1997**, *36*, 4208.

(10) Kortz, U.; Savelieff, M. G.; Bassil, B. S.; Keita, B.; Nadjo, L. *Inorg. Chem.* **2002**, *41*, 783.

(11) Tézé, A.; Vaissermann, J. *C. R. Acad. Sci., Ser. IIc: Chim.* **2000**, *3*, 101.

(12) Nozaki, C.; Kiyoto, I.; Minai, Y.; Misono, M.; Mizuno, N. *Inorg. Chem.* **1999**, *38*, 5724.

(13) Li, M.-X.; Jin, S.-L.; Liu, H.-Z.; Xie, G.-Y.; Chen, M.-Q.; Xu, Z.; You, X.-Z. *Polyhedron* **1998**, *17*, 3721.

(14) (a) Müller, A.; Luban, M.; Schröder, C.; Modler, R.; Kögerler, P.; Axenovich, M.; Schnack, J.; Canfield, P.; Bud'ko, S.; Harrison, N. *ChemPhysChem* **2001**, *2*, 517. (b) Müller, A.; Krickemeyer, E.; Das, S. K.; Kögerler, P.; Sarkar, S.; Bögge, H.; Schmidtmann, M.; Sarkar, S. *Angew. Chem., Int. Ed.* **2000**, *39*, 1612. (c) Coronado, E.; Galán-Mascarós, J. R.; Giménez-Saiz, C.; Gómez-García, C. J.; Triki, S. *J. Am. Chem. Soc.* **1998**, *120*, 4671.

(15) (a) Cavani, F.; Mezzogori, R.; Trovarelli, A. *J. Mol. Catal. A: Chem.* **2003**, *204*, 599. (b) Kuznetsova, N. I.; Kirillova, N. V.; Kuznetsova, L. I.; Likholobov, V. A. *J. Mol. Catal. A: Chem.* **2003**, *204*, 591. (c) Okun, N. M.; Anderson, T. M.; Hill, C. L. *J. Mol. Catal. A: Chem.* **2003**, *197*, 283. (d) Okun, N. M.; Anderson, T. M.; Hill, C. L. *J. Am. Chem. Soc.* **2003**, *125*, 3194. (e) Adam, W.; Alsters, P. L.; Neumann, R.; Saha-Möller, C. R.; Seebach, D.; Beck, A. K.; Zhang, R. *J. Org. Chem.* **2003**, *68*, 8222. (f) Mizuno, N.; Misono, M.; Nishiyama, Y.; Seki, Y.; Kiyoto, I.; Nozaki, C. *Res. Chem. Intermed.* **2000**, *26*, 193. (g) Mizuno, N.; Seki, Y.; Nishiyama, Y.; Kiyoto, I.; Misono, M. *J. Catal.* **1999**, *184*, 550.

(16) (a) Mbomekalle, I. M.; Keita, B.; Nadjo, L.; Berthet, P.; Hardcastle, K. I.; Hill, C. L.; Anderson, T. M. *Inorg. Chem.* **2003**, *42*, 1163. (b) Bi, L.-H.; Liu, J.-Y.; Shen, Y.; Jiang, J.-G.; Dong, S.-J. *New. J. Chem.* **2003**, *27*, 756. (c) Cheng, L.; Sun, H.-R.; Liu, B.-F.; Liu, J.-F.; Dong, S.-J. *Electrochem. Commun.* **1999**, *1*, 155. (d) Cheng, L.; Sun, H.; Liu, B.-F.; Liu, J.-F.; Dong, S.-J. *J. Chem. Soc., Dalton Trans.* **1999**, 2619. (e) Song, W.-B.; Wang, X.-H.; Liu, Y.; Liu, J.-F.; Xu, H.-D. *J. Electroanal. Chem.* **1999**, *476*, 85.

Experimental Section

Synthesis. $K_6Na_2[GeW_{11}O_{39}]\cdot 13H_2O$ was synthesized according to a published procedure, and its purity was confirmed by infrared spectroscopy.[18] All other reagents were used as purchased without further purification.

$K_8Na_2[A\text{-}\alpha\text{-}GeW_9O_{34}]\cdot 25H_2O$. A 43.5 g (13.5 mmol) sample of $K_6Na_2[GeW_{11}O_{39}]\cdot 13H_2O$ [18] was dissolved in 400 mL of water with stirring. Then 22.5 g (162.8 mmol) of K_2CO_3 was added in small portions to this solution. After stirring for about 30 min. (pH $\sim$ 9.5), a white precipitate appeared slowly. After an additional 20 min. of stirring, the white solid product was collected on a sintered glass frit, washed with saturated KCl solution (20 mL), and air-dried. Yield: 34.8 g (80%). IR for $K_8Na_2[A\text{-}\alpha\text{-}GeW_9O_{34}]\cdot 25H_2O$: 962(w), 920(m), 868(sh), 813(s), 767(sh), 695(m), 527(w), 478-(w) cm^{-1}. Anal. Calcd (found) for $K_8Na_2[A\text{-}\alpha\text{-}GeW_9O_{34}]\cdot 25H_2O$: K, 10.2 (10.0); Na, 1.5 (1.2); W, 53.7 (53.9); Ge, 2.4 (2.2).

$Cs_4Na_7[Fe_6(OH)_3(A\text{-}\alpha\text{-}GeW_9O_{34}(OH)_3)_2]\cdot 30H_2O$ (1a). A 0.15 g (0.56 mmol) sample of $FeCl_3\cdot 6H_2O$ was dissolved in 20 mL of 0.5 M NaAc buffer (pH 4.8), and then 0.52 g (0.17 mmol) of $K_8Na_2[A\text{-}\alpha\text{-}GeW_9O_{34}]\cdot 25H_2O$ was added with gentle stirring. The solution was heated to 50 °C for about 1 h and filtered after it had cooled to room temperature. Then 0.5 mL of 1.0 M CsCl solution was added to the red filtrate. Slow evaporation at room temperature led to 0.31 g (yield 58%) of a yellow crystalline product after about 1 week. IR for **1a**: 1132(w), 945(m), 876(m), 805(s), 765(s), 723-(s), 527(w), 461(w) cm^{-1}. Anal. Calcd (found) for **1a**: Cs, 8.5 (7.6); Na, 2.6 (2.1); W, 52.8 (52.9); Fe, 5.4 (5.1); Ge, 2.3 (2.1).

Elemental analysis was performed by Kanti Labs Ltd. in Mississauga, Canada. The IR spectrum was recorded on a Nicolet Avatar FTIR spectrophotometer in a KBr pellet.

X-ray Crystallography. A yellow, block-shaped crystal with dimensions $0.13 \times 0.08 \times 0.06$ mm^3 was mounted on a glass fiber for indexing and intensity data collection at 200 K on a Bruker D8 SMART APEX CCD single-crystal diffractometer using Mo Kα radiation ($\lambda = 0.710\ 73$ Å). Direct methods were used to solve the structure and to locate the tungsten atoms (SHELXS97). Then the remaining atoms were found from successive difference maps (SHELXL97). Routine Lorentz and polarization corrections were applied, and an absorption correction was performed using the SADABS program.[19] Crystallographic data are summarized in Table 1.

General Electrochemical Methods and Materials. Pure water was obtained by passing through a RiOs 8 unit followed by a Millipore-Q Academic purification set. All reagents were of high-purity grade and were used as purchased without further purification. The UV−visible spectra were recorded on a Perkin-Elmer Lambda 19 spectrophotometer on 1.6×10^{-5} M solutions of the relevant polyanion. Matched 1.000 cm optical path quartz cuvettes were used. The compositions of the various media were as follows: for pH 3, 0.2 M $Na_2SO_4 + H_2SO_4$ or 0.4 M NaY + HY (Y = Cl^-, ClO_4^-, $H_2PO_4^-$, $CH_3COO^- + ClCH_2COOH$); for pH 4 and 5, 0.4 M $CH_3COONa + CH_3COOH$; for pH 5−7, 0.4 M NaH_2PO_4 + NaOH.

Electrochemical Experiments. The same media as those for UV−visible spectroscopy were used for electrochemistry, but the polyanion concentration was 2×10^{-4} M. The solutions were deaerated thoroughly for at least 30 min. with pure argon and kept under a positive pressure of this gas during the experiments. The source, mounting, and polishing of the glassy carbon (GC, Tokai, Japan) electrodes has been described.[20] The glassy carbon samples had a diameter of 3 mm. The electrochemical setup was an EG & G 273 A driven by a PC with the M270 software. Potentials are quoted against a saturated calomel electrode (SCE). The counter electrode was a platinum gauze of large surface area. All experiments were performed at room temperature.

Table 1. Crystal Data and Structure Refinement for $Cs_4Na_7[Fe_6(OH)_3(A\text{-}\alpha\text{-}GeW_9O_{34}(OH)_3)_2]\cdot 30H_2O$ (**1a**)

emp formula	$Cs_4Fe_6Ge_2H_{69}Na_7O_{107}W_{18}$
fw	6263.9
space group	$C_{2/m}$ (No. 12)
a (Å)	36.981(4)
b (Å)	16.5759(15)
c (Å)	16.0678(15)
β (deg)	95.311(3)
vol (Å^3)	9807.1(16)
Z	4
temp (°C)	−73
wavelength (Å)	0.710 73
d_{calcd} (Mg·m^{-3})	4.102
abs coeff (mm^{-1})	24.065
$R\ [I > 2\sigma(I)]^a$	0.074
R_w (all data)^b	0.166

^{a} $R = \sum||F_o| - |F_c||/\sum|F_o|$. ^{b} $R_w = [\sum w(F_o^2 - F_c^2)^2/\sum w(F_o^2)^2]^{1/2}$.

Magnetic Susceptibility Measurements. Magnetic susceptibility measurements were carried out on powder samples of **1a** using a Quantum Design MPMS SQUID magnetometer in the temperature range of 1.8−300 K with an applied field of 0.1 T. The data were corrected for the sample holder, TIP of Fe^{3+} ions, and molecular diamagnetism which was estimated from Klemm constants.[21]

EPR Measurements. Polycrystalline powder EPR spectra of **1a** were recorded at frequencies ranging from 90 to 370 GHz at the high-field electron magnetic resonance facility at the National High Magnetic Field Laboratory in Tallahassee, FL, as described elsewhere.[22,23] Temperature variation was carried out from room temperature to 4 K. An Oxford Instruments Teslatron superconducting magnet sweepable between 0 and 17 T was used to apply the Zeeman field. In all experiments the modulation amplitudes and microwave power were adjusted for optimal signal intensity and resolution. The Bruker XSophe EPR simulation program was used with the appropriate spin Hamiltonian to generate simulated EPR spectra. This program includes a Boltzmann term that considers thermal population of particular spin levels.

Results and Discussion

Synthesis and Structure. The novel dimeric tungstogermanate $[Fe_6(OH)_3(A\text{-}\alpha\text{-}GeW_9O_{34}(OH)_3)_2]^{11-}$ (**1**) consists of two lacunary $[A\text{-}\alpha\text{-}GeW_9O_{34}]^{10-}$ Keggin moieties linked via a trigonal-prismatic $Fe_6(OH)_9$ fragment, leading to a structure with idealized D_{3h} symmetry (see Figures 1 and 2). Alternatively, the structure of **1** can be described as a Keggin dimer, formed by fusion of two hypothetical $[Fe_3(OH_2)_3(A\text{-}\alpha\text{-}GeW_9O_{34}(OH)_3)]^{4-}$ monomers. The "double-sandwich" structural type of **1** had been suggested for the first time in

(17) (a) Hervé, G.; Tézé, A. *Inorg. Chem.* **1977**, *16*, 2115. (b) Tézé, A.; Hervé, G. *J. Inorg. Nucl. Chem.* **1977**, *39*, 2151.
(18) Haraguchi, N.; Okaue, Y.; Isobe, T.; Matsuda, Y. *Inorg. Chem.* **1994**, *33*, 1015.
(19) Sheldrick, G. M. *SADABS*; University of Göttingen: Göttingen, Germany, 1996.
(20) Keita, B.; Girard, F.; Nadjo, L.; Contant, R.; Belghiche, R.; Abbessi, M. *J. Electroanal. Chem.* **2001**, *508*, 70.
(21) Vulfson, S. G. *Molecular Magnetochemistry*; Gordon and Breach Science: Amsterdam, 1998; p 241.
(22) Cage, B.; Hassan, A. K.; Pardi, L.; Krzystek, J.; Brunel, L. C.; Dalal, N. S. *J. Magn. Reson.* **1997**, *124*, 495.
(23) Hassan, A. K.; Pardi, L. A.; Krzystek, J.; Sienkiewicz, A.; Goy, P.; Rohrer, M.; Brunel, L. C. *J. Magn. Reson.* **2000**, *142*, 300.

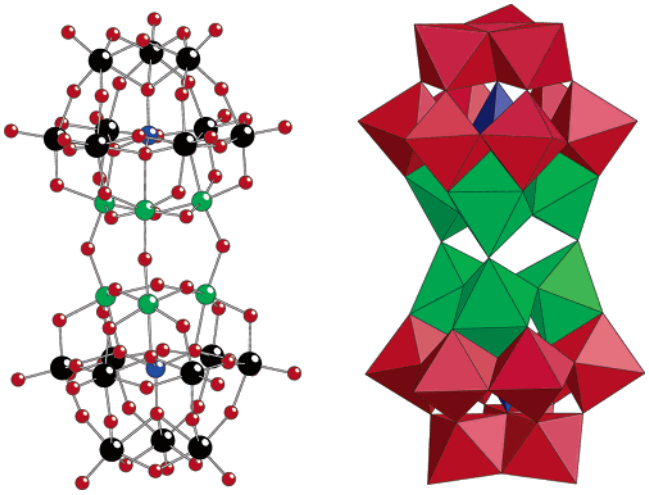

Figure 1. Ball and stick (left) and polyhedral (right) representations of $[Fe_6(OH)_3(A\text{-}\alpha\text{-}GeW_9O_{34}(OH)_3)_2]^{11-}$ (**1**). The color code is as follows: iron (green), tungsten (black), germanium (blue), and oxygen (red).

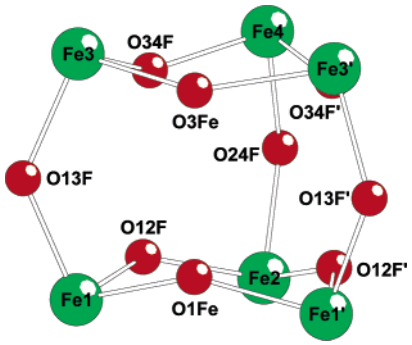

Figure 2. Ball and stick representation of the central $Fe_6(OH)_9$ fragment in **1** including the atomic labeling.

1984 by Finke *et al*. for $A\text{-}\beta\text{-}[Si_2W_{18}Nb_6O_{77}]^{8-}$ as based on solution ^{183}W NMR and FAB mass spectroscopy.[24] Some years later Pope *et al*. synthesized a series of monomeric Keggin based tungstosilicates trisubstituted by first-row transition metals, and they hinted at the possible formation of dimers by condensation.[25] In 1993, Yamase *et al*. described the crystallographic structure of $A\text{-}\alpha\text{-}[Ge_2W_{18}Ti_6O_{77}]^{14-}$, and later in the same year Finke reported on $A\text{-}\beta\text{-}[Si_2W_{18}Ti_6O_{77}]^{14-}$.[26] Two years later Lunk *et al*. synthesized the chromium(III) derivative $[\{A\text{-}\alpha\text{-}SiO_4W_9O_{30}(OH)_3Cr_3\}_2(OH)_3]^{11-}$, which represented the first example of a Keggin dimer substituted by paramagnetic transition metal ions.[27] In 1999 Hill *et al*. reported on the structure, solution properties, and antiviral activity of $A\text{-}\alpha\text{-}[Si_2Nb_6W_{18}O_{77}]^{8-}$.[28] Finally, Nomiya *et al*. characterized the first tungstophosphate derivative $A\text{-}\alpha\text{-}[P_2W_{18}Ti_6O_{77}]^{12-}$ by single-crystal X-ray analysis and also $A\text{-}\alpha\text{-}[Si_2W_{18}Ti_6O_{77}]^{14-}$ by solution ^{31}P and ^{183}W NMR studies.[29] Therefore **1** represents the iron(III) containing tungstogermanate derivative of this structural subclass, but we also prepared the analogous tungstosilicate.[30] The six FeO_6 octahedra (d^5, high spin) in **1** are corner-sharing, which leads to a central, trigonal prismatic $Fe_6(OH)_9$ fragment representing a highly attractive magnetic fragment with a possible $S = 15$ spin state. In the solid-state assembly of **1a** neighboring polyanions are oriented parallel to each other, resulting in layers in the *ac* plane that are offset to each other. However, separations of the closest magnetic Fe_6 fragments are relatively large (>7.5 Å) so that intermolecular interactions are negligible (see below). A few years ago Müller *et al*. reported on the synthesis and magnetic properties of a six-iron-substituted polyoxomolybdate with an apparent trigonal prismatic arrangement of the iron centers. However, in this case the trigonal prism is composed of two distant, eclipsed Fe_3 triangles on opposite sides of the polyoxoanion.[32]

Synthesis of **1** was accomplished in a rational, one-pot procedure by interaction of Fe^{3+} ions with the trilacunary $[A\text{-}\alpha\text{-}GeW_9O_{34}]^{10-}$ precursor in aqueous, acidic medium (pH 4.8). Interestingly, Lunk *et al*. obtained the dimeric, chromium-substituted tungstosilicate $[\{A\text{-}\alpha\text{-}SiO_4W_9O_{30}(OH)_3Cr_3\}_2(OH)_3]^{11-}$ at a similar pH (5.5), but via controlled condensation of the monomer $[A\text{-}\alpha\text{-}SiO_4W_9O_{30}(OH)_3Cr_3(OH_2)_3]^{4-}$. Until now, we have not been able to isolate the hypothetical monomeric derivative of **1**, $[Fe_3(OH_2)_3(A\text{-}\alpha\text{-}GeW_9O_{34}(OH)_3)]^{4-}$. Probably we still need to identify the optimal pH region, but we believe that in principle this monomeric species can exist in solution. This is probably not true for the related titanium-substituted derivatives $A\text{-}[Si_2W_{18}Ti_6O_{77}]^{14-}$ (see above), because all the structural results on Ti(IV)-substituted polyoxotungstates available to date suggest a very strong tendency for dimer formation.[33]

The structural details of the trigonal prismatic $Fe_6(OH)_9$ fragment of **1** are of interest (see Figure 2). Bond valence sum (BVS) calculations confirm that all oxo groups linking two iron atoms are monoprotonated.[34] As expected the Fe^{3+}

(24) Finke, R. G.; Droege, M. W. *J. Am. Chem. Soc.* **1984**, *106*, 7274.
(25) Liu, J.-F.; Ortéga, F.; Sethuraman, P.; Katsoulis, D. E.; Costello, C. E.; Pope, M. T. *J. Chem. Soc., Dalton Trans.* **1992**, 1901.
(26) (a) Yamase, T.; Ozeki, T.; Sakamoto, H.; Nishiya, S.; Yamamoto, A. *Bull. Chem. Soc. Jpn.* **1993**, *66*, 103. (b) Lin, Y.; Weakley, T. J. R.; Rapko, B.; Finke, R. G. *Inorg. Chem.* **1993**, *32*, 5095.
(27) Wassermann, K.; Palm, R.; Lunk, H. J.; Fuchs, J.; Steinfeldt, N.; Stösser, R. *Inorg. Chem.* **1995**, *34*, 5029.
(28) Kim, G. S.; Zeng, H. D.; Rhule, J. T.; Weinstock, I. A.; Hill, C. L. *Chem. Commun.* **1999**, *17*, 1651.
(29) Nomiya, K.; Takahashi, M.; Ohsawa, K.; Widegren, J. A. *J. Chem. Soc., Dalton Trans.* **2001**, 2872.
(30) We have also synthesized $[Fe_6(OH)_3(A\text{-}\alpha\text{-}SiW_9O_{34}(OH)_3)_2]^{11-}$ (**2**) which represents the isostructural Si-analogue of **1**. The synthetic procedure for **2** was analogous to **1** (see Experimental Section), but instead of $K_8Na_2[A\text{-}\alpha\text{-}GeW_9O_{34}]\cdot 25H_2O$ we used $K_{10}[A\text{-}\alpha\text{-}SiW_9O_{34}]\cdot 24H_2O$. The mixed cesium−sodium salt $Cs_4Na_7[Fe_6(OH)_3(A\text{-}\alpha\text{-}SiW_9O_{34}(OH)_3)_2]\cdot 30.5H_2O$ (**2a**) is isomorphous with **1a**. Crystal data for **2a**: $Cs_4Fe_6H_{70}Na_7O_{107.5}Si_2W_{18}$; $M = 6183.9$; monoclinic; space group $C_{2/m}$; $a = 36.904(2)$ Å; $b = 16.5445(11)$ Å; $c = 16.0388(11)$ Å; $\beta = 95.2210(10)°$; $V = 9752.0(11)$ Å^3; $Z = 4$; $T = 173$ K; $D_{calc} = 4.070$ g·cm^{-3}; μ(Mo Kα) = 23.62 mm^{-1}; 51 029 measured and 12 535 unique reflections ($R_{int} = 0.060$). Final R1 = 0.064 (wR2 = 0.137) for 11 115 observations with $F_o > 4\sigma(F_o)$, R1 = 0.074 (wR2 = 0.144) for all unique data. The CIF file of **2a** is available as Supporting Information. While this manuscript was under review, Hill *et al*. reported also on the structure of **2** (see ref 31).
(31) Anderson, T. M.; Neiwert, W. A.; Hardcastle, K. I.; Hill, C. L. *Inorg. Chem.* **2004**, *43*, 7353.
(32) Müller, A.; Plass, W.; Krickemeyer, E.; Sessoli, R.; Gatteschi, D.; Meyer, J.; Bögge, H.; Kröckel, M.; Trautwein, A. X. *Inorg. Chim. Acta* **1998**, *271*, 9.
(33) (a) Kortz, U.; Hamzeh, S. S.; Nasser, N. A. *Chem. Eur. J.* **2003**, *9*, 2945. (b) Sakai, Y.; Yoza, K.; Kato, C. N.; Nomiya, K. *Chem. Eur. J.* **2003**, *9*, 4077. (c) Sakai, Y.; Yoza, K.; Kato, C. N.; Nomiya, K. *J. Chem. Soc., Dalton Trans.* **2003**, 3581.
(34) Brown, I. D.; Altermatt, D. *Acta Crystallogr.* **1985**, *B41*, 244.

Table 2. Bond Distances (Å) and Angles (deg) for the Central $Fe_6(OH)_9$ Fragment in $[Fe_6(OH)_3(A\text{-}\alpha\text{-}GeW_9O_{34}(OH)_3)_2]^{11-}$ (**1**)

	Fe1	Fe2	Fe3	Fe4	Fe1′	Fe3′	angle Fe−O−Fe
O1Fe	1.963(7)				1.963(7)		142.3(11)
O12F	2.005(12)	2.000(12)					139.5(7)
O13F	1.949(12)		1.956(12)				131.8(6)
O3Fe			2.022(6)			2.022(6)	140.8(9)
O24F		1.939(18)		1.953(17)			134.3(9)
O34F			1.978(13)	1.974(13)			141.2(7)

ions are fairly regularly coordinated octahedrally (Fe−O, 1.949−2.172(13) Å), and the Fe−O−Fe bond angles can be subdivided in *inter*-Keggin connectivities (131.8−134.3(8)°) and *intra*-Keggin connectivities (139.5−142.3(9)°); for details see Table 2. The bond lengths and angles within the (GeW_9O_{34}) fragments of **1** are as expected.

The combination of single-crystal XRD and elemental analysis confirmed that **1** has a charge of −11. We discovered that **1a** is a mixed cesium−sodium salt, and X-ray diffraction allowed identification of all four Cs^+ ions, but only one Na^+ ion. This means that six Na^+ ions could not be located due to disorder, which is not uncommon in polyoxoanion chemistry. Nevertheless, the presence of these remaining sodium ions and therefore the entire cation composition of **1a** was fully revealed by elemental analysis.

Electrochemistry. The stability of **1** was assessed by monitoring its UV−vis spectrum as a function of pH over a period of at least 24 h. Between pH = 3 and pH = 7, all the spectra were reproducible with respect to absorbances and wavelengths. In this domain, the spectrum of **1** was characterized by a well-defined peak, the location of which varied between 258.4 and 260.5 nm when the pH increased from 3 to 7. A complementary cross-check of this suggested stability was obtained by cyclic voltammetry. In media where **1** was not stable, the spectrum associated with its gradual transformation became ill-defined. For instance, at pH 2, the peak observed initially at 256.8 nm disappeared gradually; the spectrum broadened with its maximum absorption shifted in the short-wavelength direction.

Figure 3A shows the cyclic voltammogram of **1** obtained at a scan rate of 10 mV·s^{-1}, in a pH 3 sulfate medium (0.2 M Na_2SO_4 + H_2SO_4). The pattern is restricted to the two waves, which feature respectively the reduction of Fe^{3+} centers and the first W wave. In the following, attention is focused on the reduction of Fe^{3+} centers. Its reduction peak potential is observed at $E_{pc} = -0.248$ V vs SCE. A loose comparison with the corresponding E_{pc} values for free Fe^{3+} ($E_{pc} = 0.074$ V vs SCE) and $[Fe_4(H_2O)_{10}(\beta\text{-}AsW_9O_{33})_2]^{6-}$ ($E_{pc} = -0.126$ V vs SCE) in the same electrolyte[10] supports the usual expectation that the order of peak potentials should follow the overall negative charges of the complexes, under the complementary assumption of otherwise identical influences. Whatever the scan rate from 1000 mV·s^{-1} down to 2 mV·s^{-1}, no splitting of the single Fe wave of **1** was observed. Controlled potential coulometry with the potential set at −0.400 V vs SCE indicates the consumption of 6.08 ± 0.05 electrons/molecule, thus confirming the simultaneous one-electron reduction of each of the six Fe centers. As a good piece of evidence that the tungsten−oxo framework was not reduced, the electrolysis did not give the characteristic blue

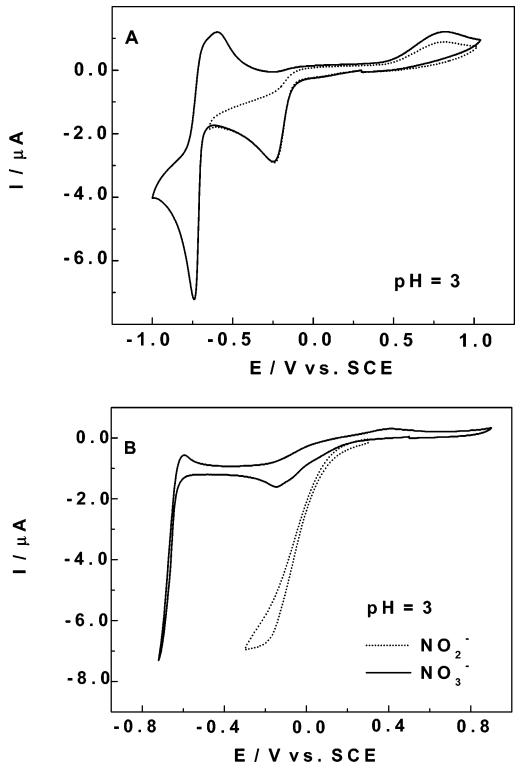

Figure 3. Cyclic voltammograms in a 2 × 10^{-4} M solution of **1a** in pH = 3 media: working electrode, glassy carbon; reference electrode, SCE. (A) pH = 3 sulfate medium (0.2 M Na_2SO_4 + H_2SO_4); superposition of the CVs restricted to the Fe wave (dotted line) and to the Fe wave and the first W redox processes (continuous line), respectively; scan rate, 10 mV·s^{-1}. (B) pH = 3 acetate medium (0.4 M CH_3COONa + $ClCH_2COOH$); superposition of the CVs run in the presence of 6 × 10^{-3} M NO_2^- and 2 × 10^{-1} M NO_3^-, respectively; scan rate, 2 mV·s^{-1}.

color. Exchange of a relatively high number of electrons in POM electrochemistry was described previously.[35,36] In cases when such exchanges are associated with proton consumption, we have shown that buffer capacity of the supporting electrolyte might influence the shape and potential location of the voltammetric waves.[35,37] In agreement with expectations from previous work,[37] the decrease in buffer capacity from SO_4^{2-} to $H_2PO_4^-$, Cl^-, and finally ClO_4^- was more and more sensitive in this order, giving a drawn out wave with a peak potential shifted in the negative direction. In contrast, the CH_3COO^- anion shows the other remarkable difference with the SO_4^{2-} medium. Three representative examples are shown in the Supporting Information: they compare the cyclic voltammograms in acetate and sulfate

(35) Keita, B.; Lu, Y.-W.; Nadjo, L.; Contant, R. *Electrochem. Commun.* **2000**, *2*, 720.
(36) Nicoara, A.; Patrut, A.; Margineanu, D.; Müller, A. *Electrochem. Commun.* **2003**, *5*, 511.
(37) Keita, B.; Lu, Y.-W.; Nadjo, L.; Contant, R. *Eur. J. Inorg. Chem.* **2000**, 2463.

media (SI1), in acetate and chloride (SI2), and in acetate and phosphate media (SI3).

In several examples, we have shown that accumulation of transition metal cation centers within POMs was favorable in electrocatalytic processes.[38,39] Therefore, the electrocatalytic behavior of **1** toward the reduction of nitrite and nitrate was tested at pH = 3. At this pH and in the potential region explored, no direct reduction of nitrite or nitrate on the glassy carbon electrode surface could be observed.[40,41] In the absence of either of the two NO_x, the voltammetric pattern is that of Figure 3A. Figure 3B sketches, in superposition, the main observations in their presence. Upon addition of even modest amounts of nitrite,[42] a large cathodic current enhancement was observed, starting in a potential domain positive to the Fe wave. This observation must be linked with the beneficial accumulation of electrons in the polyoxoanion framework.[20] We have checked that NO is also electrocatalytically reduced in the same potential domain. Concerning nitrate, it is worth reminding that a comparative study of several metal ion-substituted heteropolyanions including α_1- and α_2-$P_2W_{17}M$ and α_2-$P_2W_{15}Mo_2M$, where M = V^{4+}, Mn^{2+}, Fe^{3+}, Co^{2+}, Ni^{2+}, Cu^{2+}, Zn^{2+}, and ⟹ (where ⟹ indicates the absence of M), revealed that most polyanions, except those substituted by Cu or Ni, do not show any important electrocatalytic activity toward nitrate reduction. Specifically, Fe^{3+}-substituted heteropolyanions are not efficient in the electrocatalytic reduction of nitrate.[41a] Such an observation complies with the literature where Epstein *et al*. had shown that efficient oxidation of Fe^{2+} by nitrate necessitates a catalyst.[42] In contrast, the electrocatalytic reduction of nitrate was observed here when the first W-reduction processes were reached. Furthermore, the potential domain where this electrocatalysis was obtained is comparable with those of the best heteropolyanion-based electrocatalysts.[39] Owing to the slightly positive location of the W-wave of **1** relative to, for example, that of $[Ni_4Mn_2P_3W_{24}O_{94}]^{17-}$,[39] the electrocatalytic reduction of nitrate at pH 3 begins roughly 100 mV positive in the case of the former complex. Comparison of the nitrite and nitrate electrocatalysis patterns is enlightening: insofar as nitrite and NO are known to appear as intermediates in the reduction of nitrate on various metals, the potential locations of the corresponding waves would suggest that highly reduced species should be obtained in the electrocatalytic reduction of nitrate in the presence of **1**. Provisionally, the remarkable activity of **1** in the electrocatalytic reduction of nitrate is worth emphasizing since it constitutes the first example, to our knowledge, in which such an efficiency is demonstrated for an Fe^{3+} containing heteropolyanion. Finally, and in agreement with expectations, we have noted that **1** catalyzes also the electroreductions of dioxygen and hydrogen peroxide.

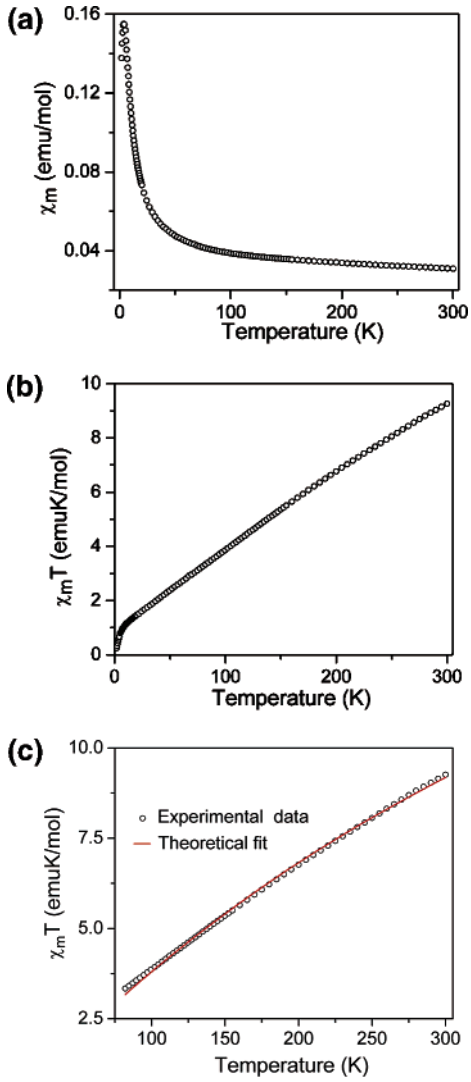

Figure 4. (a) χ_m as a function of temperature T for **1a**. (b) $\chi_m T$ vs T for **1a**. (c) $\chi_m T$ vs T for **1a** in the temperature range of 80−300 K.

Magnetic Susceptibility. The solid-state magnetic behavior of **1a** has been investigated at 0.1 T in the temperature range of 1.8−300 K. Figure 4 shows the experimental data plotted as χ_m vs T (Figure 4a) and $\chi_m T$ vs T (Figure 4b). χ_m for **1a** slowly increases from 0.031 emu·mol^{-1} at 300 K to 0.041 emu·mol^{-1} at 79.6 K, then exponentially to a maximum of 0.16 emu·mol^{-1} at 3.82 K, and followed by a decrease to 0.14 emu·mol^{-1} at 1.8 K. The decrease after 3.82 K is ascribed to intermolecular interactions. $\chi_m T$ decreases steadily from 9.26 emu·K/mol at 300 K to 0.25 emu·K/mol at 1.8 K. Comparison of the 300 K $\chi_m T$ value (9.26 emu·K/mol) to that of 26.2 emu·K/mol for a cluster of six noninteracting Fe^{3+} ($S = 5/2$) ions with $g = 2.00$ clearly points to the presence of strong antiferromagnetic spin exchange interactions between the Fe^{3+} centers and an $S_T = 0$ ground state.

(38) Keita, B.; Mbomekalle, I. M.; Nadjo, L.; Contant, R. *Electrochem. Commun*. **2001**, *3*, 267.
(39) Jabbour, D.; Keita, B.; Mbomekalle, I. M.; Nadjo, L.; Kortz, U. *Eur. J. Inorg. Chem*. **2004**, 2036.
(40) Belhouari, A.; Keita, B.; Nadjo, L.; Contant, R. *New J. Chem*. **1998**, 83.
(41) (a) Keita, B.; Abdeljalil, E.; Nadjo, L.; Contant, R.; Belghiche, R. *Electrochem. Commun*. **2001**, *3*, 56. (b) At pH = 3, the actual active species should be HNO_2 and/or NO. As a matter of fact, the following sequence is known, $HNO_2 \leftrightarrow H^+ + NO_2^-$, $pK_a = 3.3$ at 18 °C, and HNO_2 disproportionates in fairly acidic solution, $3HNO_2 \rightarrow HNO_3 + 2NO + H_2O$. The rate of this reaction is known to be slow.
(42) Epstein, I. R.; Kustin, K.; Warshaw, L. J. *J. Am. Chem. Soc*. **1980**, *102*, 3751.

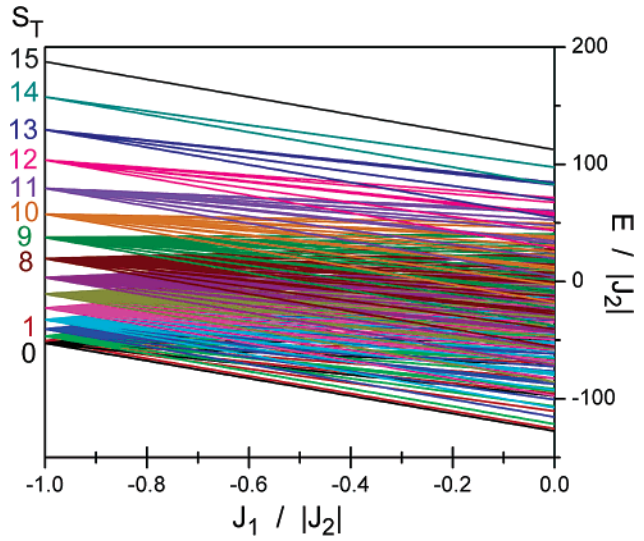

Figure 5. Spin energy spectrum of the $(Fe^{3+})_6$ cluster shown as a plot of $E/|J_2|$ vs $J_1/|J_2|$.

At the outset, neglecting the small differences in the Fe···Fe distances within each triangular unit, the Heisenberg spin exchange Hamiltonian and the corresponding eigen values for polyanion **1** are given in eq 1 and eq 2, respectively.

$$\hat{H}_{ex} = -2J_1(\hat{S}_1\cdot\hat{S}_2 + \hat{S}_{1'}\cdot\hat{S}_2 + \hat{S}_1\cdot\hat{S}_{1'} + \hat{S}_3\cdot\hat{S}_4 + \hat{S}_{3'}\cdot\hat{S}_4 + \hat{S}_3\cdot\hat{S}_{3'}) - 2J_2(\hat{S}_1\cdot\hat{S}_3 + \hat{S}_2\cdot\hat{S}_4 + \hat{S}_{1'}\cdot\hat{S}_{3'}) \quad (1)$$

$$E(S_T,S_{121'},S_{343'}) = -J_1[S_{121'}(S_{121'}+1) + S_{343'}(S_{343'}+1) - 52.5] - J_2[S_T(S_T+1) - S_{121'}(S_{121'}+1) - S_{343'}(S_{343'}+1)] \quad (2)$$

where J_1 is the *intra*trimer spin exchange constant, J_2 the *inter*trimer spin exchange constant, $\hat{S}_i$ the spin operator of the *i*th metal ion. The numbering in eq 1 corresponds to Figure 2. The above spin formalism results in 4332 different spin states ranging from a total spin of $S_T = 0-15$, in agreement with the literature.[43] A plot of $E/|J_2|$ as a function of $J_1/|J_2|$ for all the 4332 spin states is shown in Figure 5. It can be seen that the spin exchange energy levels span a continuum in the range plotted.

Analysis of the experimental magnetic susceptibility data using all of the spin states is an enormous task to undertake and beyond the scope of the present undertaking. However, we attempted to analyze the magnetic susceptibility data using a simple spin exchange model where intra- and intertrimer spin exchange constants were set equal; i.e., $J_1 = J_2 = J$. This model can be justified by taking a closer look at the Fe−O bond distances and Fe−O−Fe bond angles in polyanion **1** (cf. Table 2). The average intra- vs intertrimer Fe−O distances (∼1.99 Å vs ∼1.95 Å) demand $|J_2| \geq |J_1|$, whereas the average intra- vs intertrimer Fe−O−Fe bond angles (∼141° vs ∼133°) demand $|J_2| \leq |J_1|$.[44] Since, the difference in either Fe−O bond distances (∼0.04 Å) or Fe−O−Fe bond angles (∼8°) is not large enough for one interaction to dominate the other, it is not unreasonable to assume that they have approximately equal magnitudes. Furthermore, the Fe−O−Fe bond angles suggest that both the intra- and intertrimer spin exchange interactions are antiferromagnetic in nature.[44]

Table 3. Heisenberg Spin Exchange Energies[a] ($E(S_T)$) and Their Degeneracies

S_T	$E(S_T)$	n	S_T	$E(S_T)$	n
15	$-187.5J$	1	7	$-3.5J$	405
14	$-157.5J$	5	6	$10.5J$	505
13	$-129.5J$	15	5	$22.5J$	581
12	$-103.5J$	35	4	$32.5J$	609
11	$-79.5J$	70	3	$40.5J$	575
10	$-57.5J$	126	2	$46.5J$	475
9	$-37.5J$	204	1	$50.5J$	315
8	$-19.5J$	300	0	$52.5J$	111

[a] Energies ($E(S_T)$) are calculated from eq 3.

The assumption $J_1 = J_2$ transforms eq 2 into eq 3. The resultant energies and their degeneracies are tabulated in Table 3.

$$E(S_T) = -J[S_T(S_T+1) - 52.5] \quad (3)$$

Substitution of the energies and their degeneracies listed in Table 3 into the Van Vleck equation[45] results in

$$\chi_m = \left(\frac{10Ng^2\beta^2}{kT}\right)\left(\frac{A}{B}\right) \quad (4)$$

where N is the Avogadro number, g the Landé g-factor, β the electron Bohr magneton, k the Boltzmann constant, T the temperature in kelvin, and

$$A = 63\exp(2x) + 475\exp(6x) + 1610\exp(12x) + 3654\exp(20x) + 6391\exp(30x) + 9191\exp(42x) + 11340\exp(56x) + 12240\exp(72x) + 11628\exp(90x) + 9702\exp(110x) + 7084\exp(132x) + 4550\exp(156x) + 2457\exp(182x) + 1015\exp(210x) + 248\exp(240x)$$

$$B = 111 + 945\exp(2x) + 2375\exp(6x) + 4025\exp(12x) + 5481\exp(20x) + 6391\exp(30x) + 6565\exp(42x) + 6075\exp(56x) + 5100\exp(72x) + 3876\exp(90x) + 2646\exp(110x) + 1610\exp(132x) + 875\exp(156x) + 405\exp(182x) + 145\exp(210x) + 31\exp(240x)$$

with $x = J/kT$.

Since the ground state is diamagnetic, we were particularly interested in the high-temperature region and, as can be seen in Figure 4c, our model fits fairly well all of the high-

(43) (a) McCusker, J. K.; Christmas, C. A.; Hagen, P. M.; Chadha, R. K.; Harvey, D. F.; Hendrickson, D. N. *J. Am. Chem. Soc.* **1991**, *113*, 6114. (b) Christmas, C. A.; Tsai, H. L.; Pardi, L.; Kesselman, J. M.; Gantzel, P. K.; Chadha, R. K.; Gatteschi, D.; Harvey, D. F.; Hendrickson, D. N. *J. Am. Chem. Soc.* **1993**, *115*, 12483.

(44) (a) Kurtz, D. M., Jr. *Chem. Rev.* **1990**, *90*, 585, and references therein. (b) McCusker, J. K.; Vincent, J. B.; Schmitt, E. A.; Mino, M. L.; Shin, K.; Coggin, D. K.; Hagen, P. M.; Huffman, J. C.; Christou, G.; Hendrickson, D. N. *J. Am. Chem. Soc.* **1991**, *113*, 3012, and references therein. (c) Cañada-Vilalta, C.; O'Brien, T. A.; Brechin, E. K.; Pink, M.; Davidson, E. R.; Christou, G. *Inorg. Chem.* **2004**, *43*, 5505, and references therein.

(45) Kahn, O. *Molecular Magnetism*; VCH: New York, 1993.

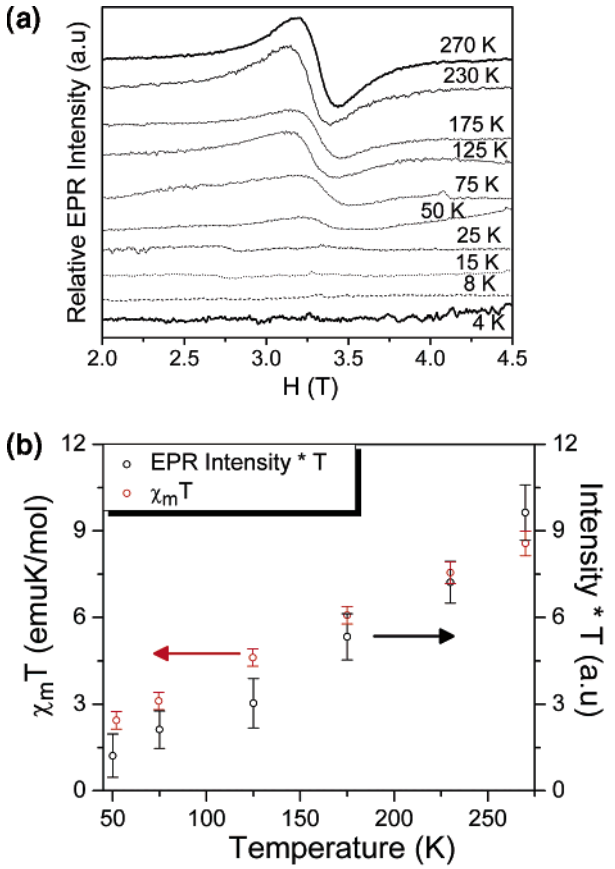

Figure 6. (a) Temperature dependence of the W band ($\nu = 92.338$ GHz) EPR of **1a**. The signal intensity decreases as the temperature is lowered, indicating a diamagnetic ground state which is EPR-silent (bottom spectrum). (b) Plot of $I_{EPR}T$ (black circles) and $\chi_m T$ (red circles) as a function of temperature (T).

temperature (80−300 K) experimental $\chi_m T$ data. The best least-squares fit, shown as the solid line in Figure 4c, yields $J = -11.5 \pm 0.2$ cm^{-1} with fixed $g = 2.0$. These results confirm the presence of an $S_T = 0$ ground state and an excited spin triplet ($S_T = 1$) ~24 cm^{-1} above the spin singlet ground state and are in agreement with other $(Fe^{3+})_6$ containing compounds reported in the literature.[44c,46,47]

EPR Spectroscopy. High-frequency EPR spectroscopy has been conducted on polycrystalline powder samples of **1a** in an effort to better understand the spin environment. One broad Lorentzian EPR transition at $g = 1.992\,51$ (isotropic) was observed at all frequencies between 90 and 370 GHz and room temperature (Figure 6a). This is expected for a high-spin Fe^{3+} ($3d^5$) center.[48] As the temperature is lowered, the EPR signal intensity drops steadily to zero, without any significant change in the peak-to-peak width, indicating that the ground state is diamagnetic, in agreement with the susceptibility analysis. The observed high-temperature signal results from low-lying paramagnetic excited spin states.

Figure 6b shows a plot of $\chi_m T$ and $I_{EPR}T$ as a function of temperature (T), assuming that the EPR intensity (I_{EPR}) is proportional to the molar susceptibility (χ_m). Though the calculated EPR intensities are approximate because of the saturation effects and lack of good line width control on the high-frequency instrument, there is a reasonable agreement between the EPR intensity and susceptibility data.

Conclusions

We have synthesized the double-sandwich POM $[Fe_6(OH)_3(A\text{-}\alpha\text{-}GeW_9O_{34}(OH)_3)_2]^{11-}$ (**1**) in aqueous, acidic medium using a simple, rational procedure. Polyanion **1** consists of two lacunary $[A\text{-}\alpha\text{-}GeW_9O_{34}]^{10-}$ Keggin moieties linked via a trigonal-prismatic $Fe_6(OH)_9$ fragment. Therefore **1** represents a Keggin dimer, and it adds an iron-containing tungstogermanate derivative to this structural subclass.

Electrochemistry studies revealed that the six Fe^{3+} centers are reduced simultaneously in most media at pH = 3. However, a partial splitting of this wave is induced in acetate buffer and also in dihydrogenphosphate medium. These observations are consistent with the expected electronic communication between the Fe^{3+} centers being superimposed on acid−base equilibria and also on the type of anions in the supporting electrolyte. The remarkable efficiency of **1** in the electrocatalytic reduction of nitrite, nitric oxide, and nitrate underscores again the usefulness of POMs substituted by multiple transition metal ions.

Our magnetic and EPR studies of **1a** indicate the presence of a diamagnetic ground state ($S_T = 0$). Analysis of the high-temperature magnetic susceptibility data, to a simple spin exchange model with J_1 (intratrimer spin exchange constant) equals J_2 (intertrimer spin exchange constant), yields $J \approx -12$ cm^{-1} with $g = 2.0$. Furthermore, our EPR intensity agrees fairly well with the molar susceptibility data.

Acknowledgment. This work was supported by the International University Bremen, the CNRS (UMR 8000), and the University Paris-Sud XI. The work at FSU was supported by NSF, DMR No. 0103290. We thank the National High Magnetic Field Laboratory (supported by NSF) for the EPR measurements. Figures 1 and 2 were generated by Diamond Version 2.1e (copyright Crystal Impact GbR).

Supporting Information Available: Two X-ray crystallographic files in CIF format; study of the electrolyte effect on the cyclic voltammetry of **1** (including three figures). This material is available free of charge via the Internet at http://pubs.acs.org.

IC048713W

(46) Representative examples include the following and references therein: (a) Micklitz, W.; Lippard, S. J. *Inorg. Chem.* **1988**, *27*, 3067. (b) Micklitz, W.; Bott, S. G.; Bentsen, J. G.; Lippard, S. J. *J. Am. Chem. Soc.* **1989**, *111*, 372. (c) Brechin, E. K.; Knapp, M. J.; Huffman, J. C.; Hendrickson, D. N.; Christou, G. *Inorg. Chim. Acta* **2000**, *297*, 389. (d) Seddon, E. J.; Huffman, J. C.; Christou, G. *J. Chem. Soc., Dalton Trans.* **2000**, 4446. (e) Murugesu, M.; Abboud, K. A.; Christou, G. *J. Chem. Soc., Dalton Trans.* **2003**, 4552.

(47) Representative examples include the following: (a) Caneschi, A.; Cornia, A.; Lippard, S. J. *Angew. Chem., Int. Ed. Engl.* **1995**, *34*, 467. (b) Caneschi, A.; Cornia, A.; Fabretti, A. C.; Foner, S.; Gatteschi, D.; Grandi, R.; Schenetti, L. *Chem. Eur. J.* **1996**, *2*, 1379. (c) Abbati, G. L.; Cornia, A.; Fabretti, A. C.; Malavasi, W.; Schenetti, L.; Caneschi, A.; Gatteschi, D. *Inorg. Chem.* **1997**, *36*, 6443.

(48) Abragam, A.; Bleaney, B. *Electron Paramagnetic Resonance of Transition Ions*; Dover: New York, 1970.